A novel heterospin polynuclear complex containing both macrocyclic and imino nitroxide radical ligands: {[CuL(H_2O)](CuL)-Mn(IM-2Py)}{[CuL(MeOH)](CuL)Mn(IM-2Py)}(ClO_4)$_4$ · MeOH

Zhi-Liang Liu,[a] Li-Cun Li,[a] Lei Zhang,[a] Dai-Zheng Liao,[a] Zong-Hui Jiang*[ab] and Shi-Ping Yan[a]

[a] *Department of Chemistry, Nankai University, Tianjin 300071, P. R. China*
[b] *State Key Laboratory of Coordination Chemistry, Nanjing University, Nanjing 210093, P. R. China*

Received (in Montpellier, France) 3rd July 2002, Accepted 18th October 2002
First published as an Advance Article on the web 10th January 2003

A novel heterospin complex containing both macrocyclic and imino nitroxide radical ligands: {[CuL(H_2O)](CuL)Mn(IM-2Py)}{[CuL(MeOH)](CuL)Mn(IM-2Py)}(ClO_4)$_4$·MeOH, has been synthesized and its crystal structure determined by X-ray diffraction methods. In order to interpret the exchange interaction of this asymmetric heterospin system which consists of two types of paramagnetic metal centers and a nitroxide radical, a theoretical model has been established. Using this theoretical model the magnetic susceptibility data have been fitted and lead to coupling constant values equal to -7.4 cm^{-1} (Mn–Rad) and -19.2 cm^{-1} (Mn–Cu), respectively.

Introduction

During the past two decades, the field of molecular magnets has attracted scientists from different fields. The major research aims in the field of molecular magnetism are on the one hand the chemical design of molecular assemblies that exhibit spontaneous magnetization and on the other hand the rationalization of magnetostructural correlation.[1] Polynuclear macrocyclic complexes and nitroxide radical metallic complexes are two active fields of research for designing and synthesizing new magnetic materials.[2–6]

Polynuclear macrocyclic complexes containing multiatomic bridges such as phenolate oxygen, oxamido and oximato groups have been considerably investigated in structural and magnetic characterizations.[7–9] Meanwhile, important results have been obtained for compounds including stable organic nitroxide radicals coordinated to paramagnetic metal ions.[10,11] Therefore, to combine the two synthetic approaches, namely, assembling complexes by nitroxide radical ligands and macrocyclic complexes containing oximato bridging groups will open one of the best strategies to design heterospin systems which consist of two types of paramagnetic metal centers and a nitroxide radical. From a magnetic point of view, some symmetric systems such as the A_3B type (Scheme 1) have been studied in detail,[12,13] but asymmetric systems such as the A_2BC model have not been studied so far.

Herein, we report a novel heterospin polynuclear complex containing different paramagnetic metal ions and imino nitroxide radicals: {[CuL(H_2O)](CuL)Mn(IM-2Py)}{[CuL-(MeOH)](CuL)Mn(IM-2Py)}(ClO_4)$_4$·MeOH derived from the precursor CuL and IM-2Py radical [L ligand is 2,3-dioxo-5,6:14,15-dibenzo-1,4,8,12-tetraazacyclopentadeca-7,12-diene, and IM-2Py stands for the 2-(2′-pyridyl)-4,4,5,5-tetramethyl-4,5-dihydro-1*H*-imidazolin-1-oxyl radical] (Scheme 2). We describe successively the synthesis, crystal structure and magnetic properties of this complex. The results of preliminary investigations into the magnetic behavior of this complex have prompted us to develop a new method to learn about the fundamental spin-coupling behavior of this asymmetric heterospin system.

A_3B
symmetric system

A_2BC
asymmetric system

Scheme 1

Experimental

Synthesis

Synthesis of the CuL precursor and IM-2Py. Diformyloxanilide was prepared according to the literature.[12–14] CuL was prepared by refluxing and stirring diformyloxanilide (0.294 g, 1 mmol), 1,3-propanediamine (0.16 ml, 2 mmol) and Cu(Ac)$_2$·H_2O (0.2 g, 1 mmol) for 2 h in 20 ml of MeOH containing 2 drops of 2 M NaOH. After cooling and filtering, a precipitate was obtained. This precipitate was then washed with water, methanol and diethyl ether successively, and dried under vacuum. Yield: 52%. Anal.: Calc. for $C_{19}H_{16}N_4O_2Cu$: C, 57.64; H, 4.07; N, 14.15; found: C, 57.32; H, 4.04; N, 14.21%. IR (KBr disc, cm^{-1}) $\nu_{C=O}$ 1640(s); $\nu_{C=N}$ 1610(w), 1590(m).

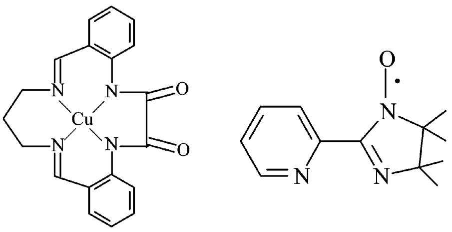

(CuL)

(IM-2Py)

Scheme 2

2-(2′-Pyridyl)-4,4,5,5-tetramethyl-4,5-dihydro-1*H*-imidazoline-1-oxyl was prepared by the literature method.[15]

Preparation of the title complex {[CuL(H_2O)](CuL)Mn(IM-2Py)}{[CuL(MeOH)](CuL)Mn(IM-2Py)}(ClO_4)$_4$ · MeOH. A solution of 10 ml MeOH containing $Mn(ClO_4)_2{\cdot}6H_2O$ (37.0 mg, 0.1 mmol) and IM-2Py (22 mg, 0.1 mmol) was added to the CuL precursor (79.0 mg, 0.2 mmol) in 30 ml MeOH under stirring and gentle heating. The mixture was further stirred for 30 min and filtered. Dark-green crystals were obtained from the filtrate after several days. IR (KBr disc, cm^{-1}): 3350 m, 2900 w, 1600 vs, 1510 m, 1450 s, 1370 w, 1080 br, 840 s, 760 m. Anal. Calc. for $C_{102}H_{106}Cl_4Cu_4Mn_2N_{22}O_{29}$: C, 46.94; H, 4.09; N, 11.80; found: C, 46.58; H, 4.21; N, 11.56%.

X-Ray analysis. Structure determination

A dark-green single crystal (0.30 × 0.25 × 0.20 mm^3) of the title complex was selected and mounted on a BRUKER SMART 1000 diffractometer equipped with graphite-monochromated MoKα radiation ($\lambda = 0.71073$ Å). The crystallographic data are given in Table 1. The high value of $R_{(\mathrm{int})}$ (0.0971) was obtained due to the disorder of some atoms in the crystal. The structure was solved with direct methods using the SHELXS-97 program.[16] O(23) (perchlorate anions) is disordered and its position was fixed. The H atoms were assigned with common isotropic displacement factors and included in the final refinement by use of geometrical restraints. The hydrogen atoms of the solvent molecules were not added. A full-matrix least-squares refinement on F^2 was carried out using the SHELXL-97 package of programs.[17]

CCDC reference number 193946. See http://www.rsc.org/suppdata/nj/b2/b206475h/ for crystallographic files in CIF or other electronic format.

Physical measurements

Elemental analyses for carbon, hydrogen, and nitrogen were carried out on a Perkin-Elmer elemental analyzer, model 240. The IR spectra were taken on a Nicolet 5DX FT-IR spectrophotometer using KBr pellets. Electronic spectrum was taken on a Shimadzu UV-2401 PC spectrophotometer in MeOH. Variable-temperature magnetic susceptibilities were measured on a Maglab system2000 magnetometer in the temperature range 2–300 K, with an applied field of 1 T. Diamagnetic corrections were made with Pascal's constants for all the constituent atoms.

Table 1 Crystallographic data and data-collection parameters for the complex

Empirical formula	$C_{102}H_{106}Cl_4Cu_4Mn_2N_{22}O_{29}$
Formula weight	2609.93
Crystal system	Triclinic
Space group	$P\bar{1}$
a/Å	14.582(4)
b/Å	15.677(5)
c/Å	25.158(8)
α/°	87.217(6)
β/°	75.768(6)
γ/°	78.204(7)
V/Å^3	5457(3)
Z	2
θ range/°	2.13 to 25.03
Index ranges	$-14 \leqslant h \leqslant 17$, $-13 \leqslant k \leqslant 18$, $-29 \leqslant l \leqslant 29$
Absorption correction	SADABS
Meas./independent refln.	22598/19081 ($R_{\mathrm{int}} = 0.0971$)
Restraints/parameters	17/1477
μ/mm^{-1}	1.176
F(000)	2676
Goodness of fit on F^2	0.937
Temperature/K	293(2)
Final R [$I > 2\sigma(I)$]	$R_1{}^a = 0.0834$, $\omega R_2{}^b = 0.1701$

^{a} $R_1 = \Sigma(||F_O| - |F_c||)/\Sigma|F_O|$. ^{b} $wR_2 = (\Sigma w(|F_O|^2 - |F_c|^2)^2/\Sigma w|F_O|^2)^{1/2}$, $w = 1/[\sigma^2(F_O{}^2) + (0.0900P)^2 + 0.0000P]$ where $P = (F_O{}^2 + 2F_c{}^2)/3$.

Results and discussion

Structure

The title complex consists of the heteronuclear complex cations {[CuL(H_2O)](CuL)Mn(IM-2Py)}$^{2+}$ and {[CuL-(MeOH)](CuL)Mn(IM-2Py)}$^{2+}$, one solvent molecule, and 4 perchlorate ions. The structure is built from two symmetrically and constitutionally independent molecules, one about atoms Mn(1), Cu(1) and Cu(2), the other about atoms Mn(2), Cu(3) and Cu(4). ORTEP drawings of the two cations are shown in Fig. 1.

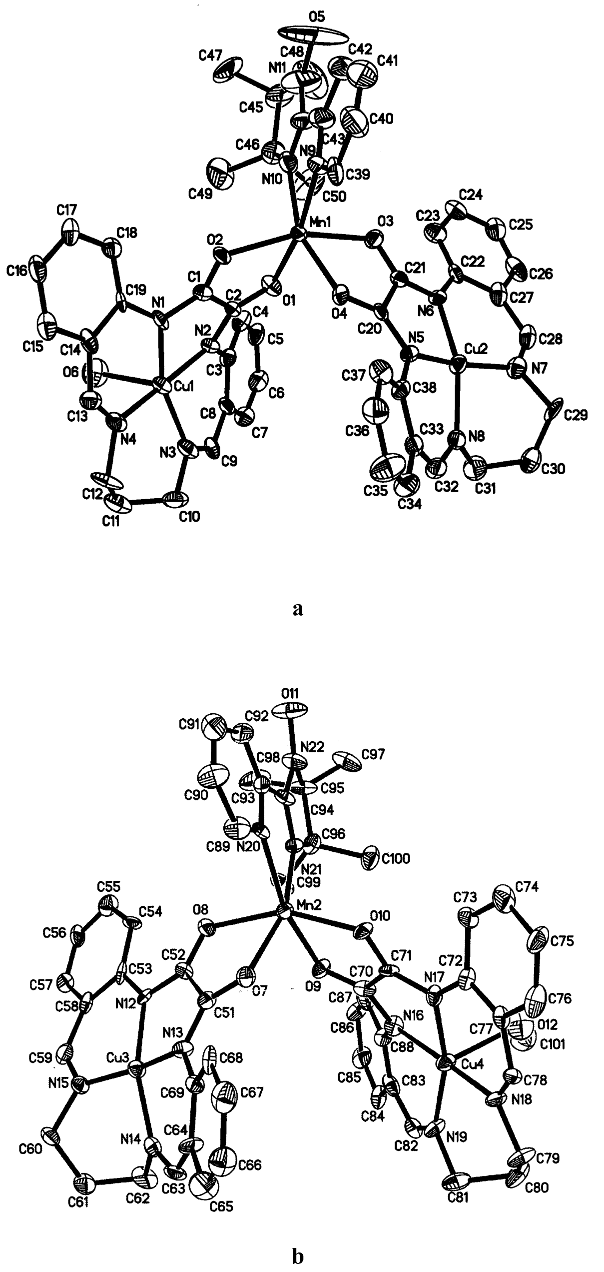

Fig. 1 ORTEP drawings of the two cations in the complex: (a) {[CuL(H_2O)](CuL)Mn(IM-2Py)}$^{2+}$ and (b) {[CuL(MeOH)](CuL)-Mn(IM-2Py)}$^{2+}$. Thermal ellipsoids are drawn at the 30% probability level.

In each of the cations, the Cu$^{\rm II}$ atoms have different coordination geometries. In cation a, Cu(2) has N_4 4-fold coordination geometry, Cu(1) has ON_4 5-fold coordination geometry due to the presence of a coordination water molecule (atom O(6) in Fig. 1a). In cation b, Cu(3) has N_4 4-fold coordination geometry, Cu(4) has ON_4 5-fold coordination geometry due to the presence of a coordination methanol molecule (atom O(12) in Fig. 1b). Cu(2) and Cu(3) display square planar coordination with the N_4 donor set from their respective macrocyclic ligands (L), the square plane in each case suffers a small tetrahedral distortion as indicated by deviations of the relevant atoms from the mean plane of the N_4 atoms (the deviations from the average planes are 0.3049 Å and 0.2803 Å, respectively). In cation a, the deviation of Cu(2) from the least-squares plane through N(5), N(6), N(7) and N(8) is 0.0538 Å; in cation b, the deviation of Cu(3) from the least-squares plane through N(12), N(13), N(14) and N(15) is −0.0632 Å. Cu(1) and Cu(4) display pyramidal coordination environments with the N_4 donor set from their respective macrocyclic ligands (L) and oxygen donor set (from water or methanol). In cation a, the deviation of Cu(1) from the least-squares plane through N(1), N(2), N(3) and N(4) is −0.2121 Å; in cation b, the deviation of Cu(4) from the least-squares plane through N(16), N(17), N(18) and N(19) is 0.1607 Å. The bond lengths of Cu(1)–O(6) and Cu(4)–O(12) are 2.360(10) and 2.347(11) Å, respectively.

The coordination environments around Mn$^{\rm II}$ are similar in cations a and b. The Mn$^{\rm II}$ ion is hexacoordinated by two nitrogen atoms of the IM-2Py ligand and by four oxygen atoms of two different oximido macrocyclic ligands, and the coordination octahedron is severely distorted. The Cu$^{\rm II}$ atom is connected to the Mn$^{\rm II}$ *via* the *exo-cis* oxygen atoms of the oxamido macrocyclic ligands. In cation a, the distances between Mn$^{\rm II}$ and Cu$^{\rm II}$ are 5.384 and 5.407 Å, respectively. In cation b, the distances between Mn$^{\rm II}$ and Cu$^{\rm II}$ are 5.389 and 5.453 Å, respectively. Selected bond lengths and angles are given in Table 2. In cation a, the dihedral angle between the planes which share the C(1)–C(2) (or C(20)–C(21)) bond of the oxamido group is 17.9° (or 22.8°). In cation b, the dihedral angle between the planes which share the C(51)–C(52) (or C(70)–C(71)) bond of the oxamido group is 18.3° (or 14.8°). The sum of the angles around the amidate nitrogen atoms of the oxamido macrocyclic ligand is very close to 360°. This fact, together with the values of the bond lengths involved and the planarity of the oxamido skeleton, reveals that the amidate nitrogens are sp^2 hybridized and that the π-carbonyl electrons are delocalized to form a conjugated system.

Spectroscopic characterization

The IR spectra of the title complex show two strong bands at *ca.* 1600 cm^{-1} and 1450 cm^{-1}, attributed to the ν(N–C–O) stretching band, which are characteristic of the bridging oxamido group,[13] the band around 1370 cm^{-1} can be assigned to the vibration of the O–N moiety of the IM-2Py ligand and a broad strong band at *ca.* 1080 cm^{-1} is characteristic of perchorate ions.[18,19]

The electronic absorption spectrum of the complex in MeOH below 400 nm is dominated by intense bands due to intraligand and charge-transfer transitions in the Cu(II) chromophore.[5] In the 500–900 nm region, relatively strong bands centered at 510–532 nm are attributed to the spin allowed d–d transitions of Cu(II) in an environment close to square planar.[13] The coordination environment of manganese(II) in the complex is a distorted octahedron. Thus, the ground state of manganese(II) is $^6A_{1g}$ according to ligand field theory. Assuming Mn$^{\rm II}$ has O_h symmetry, d–d transitions of manganese(II) ($^6A_{1g} \rightarrow {}^4T_{1g}(G)$, $^4T_{2g}(G)$, $^4A_{1g}$ ...) are spin forbidden; no characteristic band of manganese(II) was found in the spectra of the complex.[20]

Table 2 Selected bond lengths (Å) and bond angles (°) of the title complex

Cu(1)–N(1)	1.988(11)	Cu(1)–N(2)	1.997(10)	Mn(1)–O(3)	2.172(8)
Cu(1)–N(4)	1.999(12)	Cu(1)–N(3)	2.038(12)	Mn(1)–O(1)	2.182(8)
Cu(1)–O(6)	2.360(10)	Cu(2)–N(5)	1.934(10)	Mn(1)–O(4)	2.211(8)
Cu(2)–N(7)	1.916(11)	Cu(2)–N(6)	1.942(10)	Mn(2)–O(10)	2.152(8)
Cu(2)–N(8)	1.946(12)	Cu(3)–N(13)	1.920(10)	Mn(2)–O(9)	2.185(8)
Cu(3)–N(15)	1.917(10)	Cu(3)–N(12)	1.934(9)	Mn(2)–O(7)	2.231(9)
Cu(3)–N(14)	1.952(12)	Cu(4)–N(16)	1.975(10)	Mn(2)–O(8)	2.164(8)
Cu(4)–N(18)	1.987(11)	Cu(4)–N(17)	2.001(10)	Mn(2)–N(21)	2.200(10)
Cu(4)–N(19)	2.027(11)	Cu(4)–O(12)	2.347(11)	Mn(2)–N(20)	2.291(10)
Mn(1)–N(10)	2.206(13)	Mn(1)–O(2)	2.169(8)	Mn(1)–N(9)	2.268(12)
N(11)–O(5)	1.29(2)	N(22)–O(11)	1.306(14)		

N(1)–Cu(1)–N(2)	82.3(4)	N(1)–Cu(1)–N(4)	90.1(5)
N(2)–Cu(1)–N(3)	88.6(4)	N(4)–Cu(1)–N(3)	96.8(5)
N(1)–Cu(1)–O(6)	102.0(4)	N(2)–Cu(1)–O(6)	95.1(4)
N(5)–Cu(2)–N(7)	164.7(4)	N(5)–Cu(2)–N(6)	86.4(4)
N(7)–Cu(2)–N(6)	94.6(5)	N(6)–Cu(2)–N(8)	158.1(4)
N(13)–Cu(3)–N(15)	166.9(4)	N(13)–Cu(3)–N(12)	86.0(4)
N(15)–Cu(3)–N(14)	90.5(5)	N(12)–Cu(3)–N(14)	159.3(4)
N(16)–Cu(4)–N(18)	172.9(4)	N(17)–Cu(4)–N(19)	164.1(4)
N(18)–Cu(4)–N(17)	92.6(4)	N(16)–Cu(4)–N(19)	88.2(4)
N(16)–Cu(4)–O(12)	93.1(4)	N(18)–Cu(4)–O(12)	92.1(4)
O(3)–Mn(1)–O(2)	161.2(3)	O(2)–Mn(1)–N(9)	100.3(4)
O(2)–Mn(1)–O(1)	76.0(3)	N(10)–Mn(1)–N(9)	72.7(5)
O(2)–Mn(1)–N(10)	105.5(4)	O(1)–Mn(1)–N(10)	98.4(4)
O(3)–Mn(1)–O(4)	74.0(3)	O(4)–Mn(1)–N(9)	95.6(4)
O(10)–Mn(2)–O(9)	75.1(3)	O(8)–Mn(2)–O(9)	91.1(3)
O(10)–Mn(2)–N(21)	110.8(3)	O(8)–Mn(2)–N(21)	89.8(3)
O(9)–Mn(2)–N(21)	94.0(3)	O(10)–Mn(2)–O(7)	87.2(3)
O(8)–Mn(2)–O(7)	73.4(3)	O(9)–Mn(2)–O(7)	93.2(3)
N(21)–Mn(2)–O(7)	161.8(3)	O(10)–Mn(2)–N(20)	101.1(3)
N(21)–Mn(2)–N(20)	72.6(4)	O(7)–Mn(2)–N(20)	102.2(3)

Magnetic behavior

The temperature dependence of the magnetic susceptibility for the complex was investigated in the temperature range 2–300 K, with an applied field of 1 T. The plots of $\chi_M T$ (and χ_M) *vs.* T, where χ_M is the molar magnetic susceptibility corrected for the core diamagnetism and T is temperature, are shown in Fig. 2. The $\chi_M T$ value per molecule is equal to 4.56 cm^3 K mol^{-1} at 300 K; the value is lower than the spin only value expected for one $S = 5/2$ (Mn^{II}), two $S = 1/2$ (Cu^{II}) and one $S = 1/2$ (radical) uncorrelated spins (5.50 cm^3 K mol^{-1}) indicating the presence of antiferromagnetic interactions between the spin carriers.

For the present complex, the four-spin system is asymmetric from a magnetic point of view. The spin Hamiltonian that fully describes the situation of this system can be given as $\hat{H} = -2J_{MnCu}\hat{S}_{Mn}(\hat{S}_{Cu1} + \hat{S}_{Cu2}) - 2j_{MnR}\hat{S}_{Mn}\hat{S}_R$, where J_{MnCu} and j_{MnR} characterize the exchange interactions for Mn–Cu and Mn–radical, respectively. In order to define accurately the energy level of the system, a 48 × 48 matrix should be diagonalized, and the solution to this question is quite complicated. However, the nature of the experimental data allows us to make some simplifications to the above question and still interpret the magnetic data in a meaningful fashion. Being enlightened by Miller,[21] a simple model can be established to evaluate quantitatively the magnitude of the spin exchange interactions in the four-spin asymmetric system (Scheme 3).

In this model, first, we consider Mn–radical as a fragment having coupling states of $S = 2$ and $S = 3$. The populations of each state at various temperatures can be derived:

$$P_{(S=2)} = \frac{5\exp(-6j/KT)}{7 + 5\exp(-6j/KT)} \tag{1}$$

$$P_{(S=3)} = \frac{7}{7 + 5\exp(-6j/KT)} \tag{2}$$

where j represents the Mn–radical interaction. Second, we can evaluate the interactions of each states of the fragment with the two Cu^{II} using the spin Hamiltonians $\hat{H}' = -2J(\hat{S}_{(2)}\hat{S}_{Cu1} + \hat{S}_{(2)}\hat{S}_{Cu2})$ and $\hat{H}'' = -2J(\hat{S}_{(3)}\hat{S}_{Cu1} + \hat{S}_{(3)}\hat{S}_{Cu2})$: $\hat{S}_{(2)}$ and $\hat{S}_{(3)}$ represent the spin operators of the coupling states of $S = 2$ and $S = 3$, respectively. The coupling constant (J) is the average of the interactions between Cu^{II} and the different coupling states. Assuming $g_{Mn} = g_{Cu} = g_R = g$ to simplify the question and using the Van Vleck equation results in eqn. 3 and eqn. 4 to express the magnetic susceptibilities of each of the coupling states and two Cu(II), respectively:

$$\chi_M{}' = \frac{Ng^2\beta^2}{KT} \times \left(\frac{28\exp(10J/KT) + 10\exp(4J/KT) + 2 + 10\exp(6J/KT)}{7\exp(10J/KT) + 5\exp(4J/KT) + 3 + 5\exp(4J/KT)}\right) \tag{3}$$

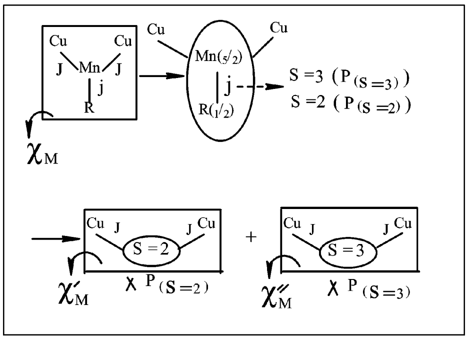

Scheme 3

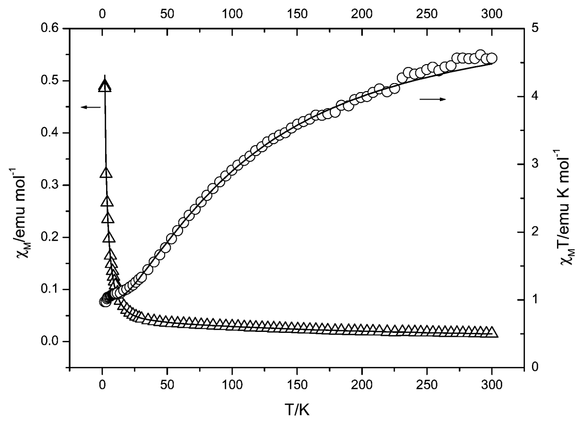

Fig. 2 The χ_m and $\chi_m T$ *versus* T plots of the complex, the solid lines show the fitting values.

$$\chi_M{}'' = \frac{Ng^2\beta^2}{KT} \times \left(\frac{60\exp(14J/KT) + 28\exp(6J/KT) + 10 + 28\exp(8J/KT)}{9\exp(14J/KT) + 7\exp(6J/KT) + 5 + 7\exp(8J/KT)}\right) \tag{4}$$

where J is the exchange interaction between the fragment ($S = 2$ or $S = 3$ state) and Cu^{II}. Last, the total magnetic susceptibility of the system (χ_M) can be obtained from eqn. 5:

$$\chi_M = \chi_M{}' \times P_{(S=2)} + \chi_M{}'' \times P_{(S=3)} \tag{5}$$

The calculated fit of the experimental data using eqns. 1–5 is shown as a solid line in Fig. 2. Fitting over the entire temperature range yields $J = -19.2$ cm^{-1}, $j = -7.4$ cm^{-1} and $g = 2.01$; agreement factor $R = \Sigma[(\chi_M)_{obs} - (\chi_M)_{calc}]^2/\Sigma[(\chi_M)_{obs}]^2 = 3.2 \times 10^{-4}$.

The small negative j value implies a weak antiferromagnetic interaction between Mn^{II} and the radical. This agrees with reported Mn^{II}–imino nitroxide complexes exhibiting antiferromagnetic exchange couplings between Mn^{II} and the radical.[22] The antiferromagnetic exchange coupling is mainly because of the orbital overlap between the π* molecular orbital of the IM-2Py and the metal d_{xy}, d_{xz} or d_{yz} orbitals. Due to the high electronegativity of oxygen resulting in the lower spin density of the imidazoline nitrogen which is connected to Mn^{II}, the overlap is accordingly small and the exchange coupling is weak. According to Kahn,[3] the antiferromagnetic interaction between Cu(II) and Mn^{II} arises from the non-zero overlap between the d_{z^2} or $d_{x^2-y}{}^2$ magnetic orbitals centered on the two metal ions and delocalized towards the ligands. The larger the overlap, the stronger the antiferromagnetic interaction. This may be explained on the basis of structural distortion, in this regard, one of the relevant factors is the value of the dihedral angle (γ) between the mean equatorial plane of the metal ion and the oxamido plane:[23,24] the greater the value of γ, the weaker the antiferromagnetic coupling. The relatively large γ value (15–19°) of this complex results in weak antiferromagnetic coupling between Cu(II) and Mn^{II}.[23]

Conclusion

Our results suggest that the introduction of radicals into polynuclear complexes provides a new route to design heterospin complexes which consist of two types of paramagnetic metal centers and a nitroxide radical. Meanwhile, in order to interpret the exchange interaction of this heterospin system, a theoretical model has been established. Using this theoretical model the magnetic susceptibility data have been fitted and lead to coupling constant values equal to −7.4 cm^{-1} (Mn–Rad) and −19.2 cm^{-1} (Mn–Cu), respectively. The fitting results indicate that the theoretical model is reasonable to evaluate the magnetic properties and magnitude of the heterospin system.

Acknowledgements

We acknowledge the National Natural Science Foundation of China (Nos. 20171025 and 90101028), for their generous financial support of this research.

References

1 O. Kahn, *Molecular Magnetism*, VCH, New York, 1993.
2 J. S. Miller and A. J. Epstein, *Chem. Commun.*, 1998, 1319.
3 O. Kahn, *Adv. Inorg. Chem.*, 1995, **41**, 179.
4 K. E. Vostrikova, D. Luneau, W. Wernsdorfer, P. Rey and M. Verdaguer, *J. Am. Chem. Soc.*, 2000, **122**, 718.
5 E.-Q. Gao, W.-M. Bu, G.-M. Yang, D.-Z. Liao, Z.-H. Jiang, S.-P. Yan and G.-L. Wang, *J. Chem. Soc., Dalton Trans.*, 2000, 1431.
6 K. Fegy, D. Luneau, T. Ohm, C. Paulsen and P. Rey, *Angew. Chem., Int. Ed.*, 1998, **37**, 1270.
7 P. A. Vigato, M. Tamburini and D. E. Fenton, *Coord. Chem. Rev.*, 1990, **25**, 106.
8 S. Mohanta, K. K. Nanda, R. Werner, W. Haase, A. K. Mukherjee, S. K. Dutta and K. Nag, *Inorg. Chem.*, 1997, **36**, 4656.
9 Z.-Y. Zhang, D.-Z. Liao, Z.-H. Jiang, S.-Q. Hao, X.-K. Yao, H.-G. Wang and G.-L. Wang, *Inorg. Chim. Acta*, 1990, **173**, 201.
10 K. Inoue and H. Iwamura, *J. Am. Chem. Soc.*, 1994, **116**, 3173.
11 H. O. Stumph, L. Ouahab, Y. Pei, D. Grandjean and O. Kahn, *Science*, 1993, **261**, 447.
12 J. L. Sanz, R. Ruiz, A. Gleizes, F. Lloret, J. Faus, M. Julve, J. J. Borras-Almenar and Y. Journaux, *Inorg. Chem.*, 1996, **35**, 7384.
13 F. Lloret, Y. Journaux and M. Julve, *Inorg. Chem.*, 1990, **29**, 3967.
14 L. I. Smith and J. W. Opie, *Org. Synth., Coll. Vol.*, 1995, **3**, 56.
15 J. N. Helbert, P. W. Kopf, E. H. Poindexter and B. E. Wagner, *J. Chem. Soc., Dalton Trans.*, 1975, 998.
16 G. M. Sheldrick, SHELXS-97: Program for the Solution of Crystal Structures, University of Göttingen, Germany, 1997.
17 G. M. Sheldrick, SHELXL-97: Program for the Refinement of Crystal Structures, University of Göttingen, Germany, 1997.
18 E. F. Ullman, L. Call and J. H. Osiecki, *J. Org. Chem.*, 1970, **35**, 3623.
19 K. Nakamoto, *Infrared and Raman Spectra of Inorganic and Coordination Compounds*, 5th edn., John Wiley, New York, 1997, Part B, p. 83.
20 D.-Z. Liao, J. Shi, Z.-H. Jiang, S.-P. Yan, P. Cheng and G.-L. Wang, *Polyhedron*, 1992, **11**, 2621.
21 R. E. Del. Sesto, A. M. Arif and J. S. Miller, *Inorg. Chem.*, 2000, **39**, 4894.
22 P. Rey, D. Luneau and A. Cogne, in *Magnetic Molecular Materials*; eds. D. Gatteschi, O. Kahn, J. S. Miller and F. Palacio, NATO ASI Series, Kluwer, Dordrecht, The Netherlands, 1991, vol. 198, pp. 203–214.
23 S. Alvarez, E. Julve and M. Verdaguer, *Inorg. Chem.*, 1990, **29**, 4500.
24 J. L. Sanz, B. Cervera, R. Ruiz, C. Bois, J. Faus, F. Lloret and M. Julve, *J. Chem. Soc., Dalton Trans.*, 1996, 1359.